EPJ manuscript No.
(will be inserted by the editor)

Control of cavity solitons and dynamical states in a monolithic vertical cavity laser with saturable absorber

Special Issue on Dissipative Optical Solitons

T. Elsass, K. Gauthron, G. Beaudoin, I. Sagnes, R. Kuszelewicz, and S. Barbay

Laboratoire de Photonique et de Nanostructures, CNRS-UPR20, Route de Nozay, 91460 Marcoussis, France, e-mail: sylvain.barbay@lpn.cnrs.fr

the date of receipt and acceptance should be inserted later

Abstract We present recent experimental results on the control and dynamics of cavity solitons in a monolithic, vertical cavity surface emitting laser with saturable absorber. On one hand, the fast and independent manipulation of two laser cavity solitons is achieved and a flip-flop operation is demonstrated with a single control-beam. On the other hand, a pulsing localized structure is presented and we demonstrate the control of a pulsing multispot structure that we can switch-on and off. These results are promising in view of the obtainment of a pulsed and monolithic cavity soliton laser.

PACS. 42.65.Tg Optical solitons; nonlinear guided waves – 42.65.Pc Optical bistability, multistability, and switching, including local field effects – 42.55.Sa Microcavity and microdisk lasers – 42.60.Gd Q-switching

1 Introduction

Large aspect ratio lasers with saturable absorbers are good candidates for the formation of laser cavity solitons (CSs). Laser CSs are bistable, self-localized laser spots that can be independently ignited and manipulated in the transverse plane of a nonlinear cavity. They have been reported in vertical cavity configurations in semiconductor optical amplifiers above threshold [1] and in extended cavity configurations with a coupled-cavity scheme involving a saturable absorber [2] or a frequency-selective feedback scheme with a grating [3]. In a recent paper [4] we demonstrated the formation and fast switching on and off of a single localized state in a monolithic, vertical cavity laser with saturable absorber. Spontaneous formation of multispot structures was also observed. In the latter three systems there is no coherent injection involved (no holding beam) and localized states appear as bright lasing spots on top of a low-intensity (non-lasing), uniform background. Using the same monolithic configuration, we are now able to demonstrate the independent control of two bistable and self-localized states, in a fast sequence.

In addition to be very simple, compact and not requiring any external coherent injection, which can reveal very important with respect to possible applications to all-optical processing of information, this system is also very interesting for other aspects. As an example, in above-threshold optical amplifiers, the uniform background on which CS form has a non-zero intensity and can be Hopf unstable. This is of course undesirable and limits the stability range for which CS are stable. In laser systems, this background is the stable non-lasing state, and the contrast for optical structures depends only on the amount of spontaneous emission in the non-lasing state. Moreover, microcavity systems are essentially single longitudinal-mode systems and as such are much simpler to capture with a model. Existence and basic properties (writing, erasure) of cavity solitons in microcavity lasers with saturable absorbers have been studied in [5,6,7]. It has also been theoretically found in some parametric regions that cavity soliton lasers can lead to self-pulsing cavity solitons [8], an interesting prospect from both theoretical and experimental point of views.

In the following we present recent experimental results obtained in a monolithic, vertical cavity surface emitting laser with saturable absorber. The original cavity design allowing the simultaneous presence of a gain and a saturable absorption regions inside a microcavity will be presented in section 2. In section 3 we present the fast independent on and off switching of two localized states while observations of single, self-localized and self-pulsing states are described in section 4. Finally we conclude and give perspective to this work in section 5.

2 Cavity design

The realization of an integrated laser source comprising an absorptive nonlinearity presents an interest not only for the present study but also in the framework of fabricating a compact source of light pulses. In the latter case, a Q-switching instability is sought and short pulses have

been obtained in electrically injected devices [9,10]. Both these demonstrations relied on a complex design and a complex technology in which the saturable absorber consists of a quantum-well placed either in the upper mirror stack or inside a second cavity coupled to the other one where the gain medium resides. The main challenge is to position the gain and absorption elements in close regions with maximum interaction with the electric field at cavity resonance while pumping one of them and not the other one. We have developed an alternative approach in which we use optical pumping. While the advent of cheap, and high-power pump sources makes it possible to optically pump large areas and potentially obtain high output powers, optical pumping allows one to use the coherent properties of the pump source to design a compact and monolithic cavity for self-pulsing or bistable lasers. This design relies on the technique we introduced in [11] where we showed that efficient optical pumping of broad area devices could be obtained by carefully designing the multilayer mirrors comprising the cavity of the semiconductor laser with the adoption of the design techniques developed for dielectric coatings. This is made possible thanks to the ever increasing mastering of semiconductor growth technologies. An optimization algorithm is used to design the multilayer stacks and the resulting layer thicknesses are no more quarter-wave depending on the targeted properties of the final design. The method works as follows : first of all a set of properties for the final cavity is chosen. These properties are specified either in terms of the reflectivity, transmittance or absorption spectra, or more globally, e.g. the total pump absorbed in the structure, or even in terms of field intensity at given locations inside the structure. In our case, we require that a pump window exist around the targeted pump wavelength (800nm), i.e. : we require low transmittance of the back mirror at this wavelength. The main idea being that a pumping window is created in the cavity spectrum in which, over a sufficiently large band, the pump is absorbed in the active region and reflected by the bottom mirror of the microcavity so as to avoid heating as much as possible. Two quantum wells are used for the gain section and one quantum well is used for the saturable absorber section. We aim at having a high pumping efficiency of the gain medium, while having no pump at all at the saturable absorber quantum wells. This is accomplished first by using different barrier materials for the gain and saturable absorber quantum wells (Fig. 1), and second by requiring that the pump field be almost zero at the SA quantum well location.

In addition, the back and front mirror reflectivities are targeted to be respectively 1 and 0.995 around the cavity resonance wavelength at 980nm. The back and front mirrors are composed of 79 and 50 layers respectively. All these requirements are translated mathematically by introducing a distance function measuring the departure from the ideal properties of the stack and the calculated ones for a given set of parameters. Summing all the contributions together into a single function depending on the variable parameters in the problem (here the layer thicknesses), the ideal stack is approached by a minimization

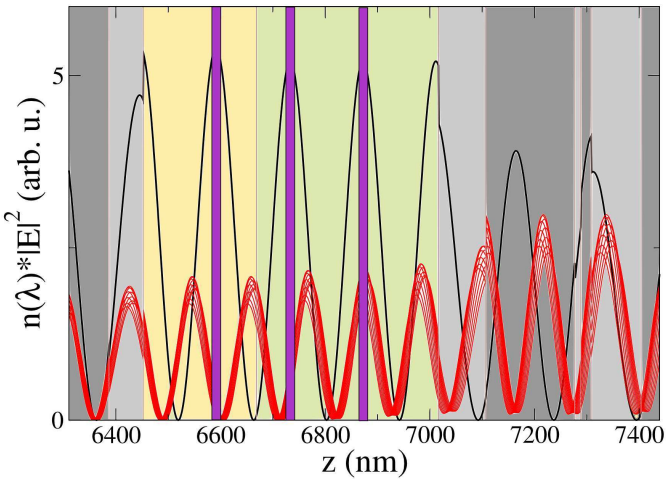

Figure 1. Active zone of the VCSEL-SA and field intensities at the cavity resonance (black, divided by 400) and at the pump wavelengths (in red, between 795nm and 805 nm) versus the growth depth. The active zone is composed of two regions (in yellow and green) : the SA region (yellow) with one $InGaAs/Al_{0.22}Ga_{0.78}As$ quantum well and the green one with two $InGaAs/Al_{0.05}Ga_{0.95}As$ quantum wells. The first few layers composing the the front and back mirrors is visible on the right and left resp. of the active zone. Light grey : AlAs. Dark Grey : $Al_{0.22}Ga_{78}As$. Note that the SA quantum well is at a node of the pump fields in the whole range of possible pump wavelength while being at an anti-node of the field at cavity resonance.

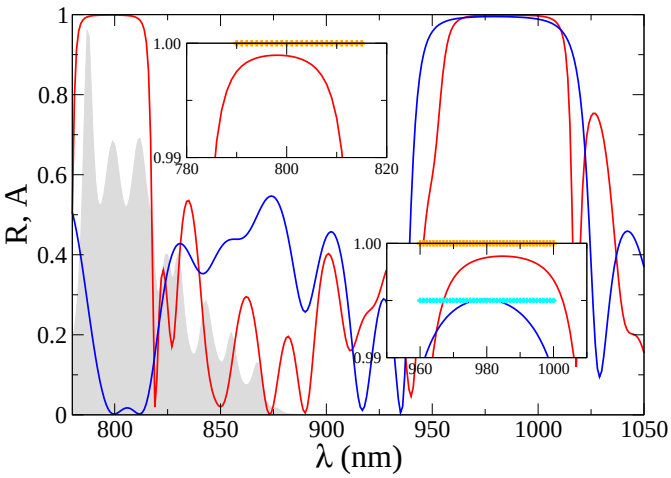

Figure 2. Calculated reflection spectra $R(\lambda)$ for the back (red) and front (blue) multilayer mirrors. The orange (resp. cyan) crosses indicate the requested reflectivities for the back (resp. front) mirror. Absorption $A(\lambda)$ in the barriers of the quantum wells appears in grey. The sought cavity resonance is 980nm and the pumping window extends around 800nm.

of this function. A standard Simplex algorithm is used to perform the optimization in this high-dimensional space. The results are presented in Fig. 2.

The structure has then been grown by metal-organic chemical vapor deposition (MOCVD). The reflectivity spectrum measured on the grown sample is presented in Fig.3.

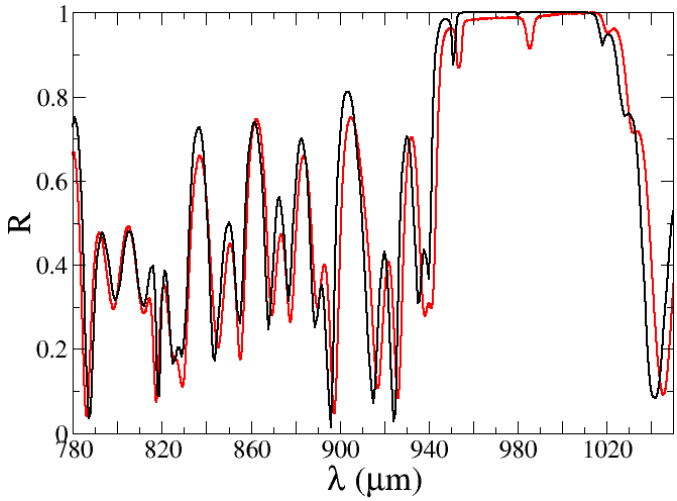

Figure 3. Comparison of the optimized calculated reflectivity spectrum (black) and the one measured experimentally (red). Note the pump window around 780-820 nm and the cavity resonance wavelength at 980nm.

There is a very good agreement between the calculated and the measured reflectivity spectrum over the whole wavelength range considered. This constitutes a very good indication that the sought parameters have been indeed very closely approached, in spite of the fact that a direct measurement of the individual parameters of the cavity (reflectivity of the mirrors, absorption, intracavity fields) would be very difficult to realize.

3 On and off switching of two cavity solitons in a fast sequence

Theoretical and numerical modelling of laser cavity solitons [5,6] indicate that stable structures can be obtained for nearly identical quantum wells in the gain and saturable absorber sections. Individual characterization of the quantum wells grown in our structure have been realized by time-resolved photo-luminescence measurements and gave non-radiative recombination times of 1.2ns and 1.6ns for the gain and saturable absorber sections respectively. This sample has been used to demonstrate the fast on and off switching of single localized states [4]. Using the same experimental set-up, we now demonstrate individual manipulation of two cavity solitons in a fast sequence. The experimental set-up is described in [4]. The sample is optically pumped with a 90μm diameter, top-hat shaped, spot. Local excitation is provided by a pulsed Ti:Sa laser with 60ps pulse duration and a variable repetition rate thanks to an acousto-optic modulator placed at the cavity output that acts as a pulse selector. The pulse is focused onto the sample down to 10μm. The wavelength of the local excitation is far from cavity resonance ($\sim 800nm$ versus 980nm) and provides a local perturbation in the pumped zone. It is an incoherent process that creates locally additional carriers. When the broad optical pump is varied, two localized states spontaneously appear in the system (Fig. 4d). Their pinning positions are certainly determined by small inhomogeneities in the sample as is very often observed in such systems. When the pump is decreased, a hysteresis is present and the two spots switch off at a lower pump value than the one at which they switched on indicating the presence of bistability. Starting from the laser off state of the system, we position the local excitation close to one of the spots (actually the local excitation spot is slightly displaced from the center of the structures to avoid perturbing the two structures at the same time). A fast photodetector is used to individually monitor the intensity at each LS site, along with the local excitation pulse taken at the output of the pulsed laser. The repetition rate of the excitation pulse is $1kHz$. On Fig.4 we show the results of these repetitive writing-erasure processes with different positions of the local excitation and of the initial conditions. In Fig.4a), the left spot is successively switched on and off while the right spot state is kept unchanged. The same operation can be done while the right spot has been initially switched on Fig.4d). Moving the local excitation spot towards the left spot, it is now possible to successively switch on and off the left spot while keeping the right spot switched off. This is a clear demonstration of independent manipulation of two spots, done for the first time in a fast sequence. Indeed in all previous experiments of this kind, and in particular in [3,2], the sequence was done by manually changing the local excitation position and only very low switching rates were demonstrated. While it was not attempted in the present experiment, we recall that in [4] the switching of an individual spot was demonstrated up to a 80MHz rate and we can presume that the same performance could be obtained here. This demonstration also completely qualifies the observed spots as cavity solitons in the sense commonly accepted in the community (bistable, self-localized spots that can be independently written and erased).

If the local perturbation is now positioned between the two spots (in fact slightly below for practical reasons, but this should not have any major physical significance), it is possible to excite both spots as shown in Fig.5. Then each time a pulse excites the CSs, their states are changed in an independent manner. If, e.g., both CSs are in the same state initially, each time a local excitation is sent each CS's state changes synchronously. Similarly, if CSs have initially opposite states, the effect of a pulse is to swap both states and the final states of CSs remain opposite. The excitation of two CSs with a single spot should imply the creation of a structure at the perturbation location followed by a drift towards the pinning positions. However, since the distance between the two spot pinning positions is of the same order as the local perturbation size (the size of the local perturbation is about 10μm and carriers can be excited on an even greater diameter), we don't expect to be able to show clear evidence for such a drift.

It is interesting to note here that the two structures are relatively close one to another, and this does not prevent their independent manipulation. Theoretically in [6] it was noted that in order for two CSs to be independently manipulable, their minimal distance was to be at

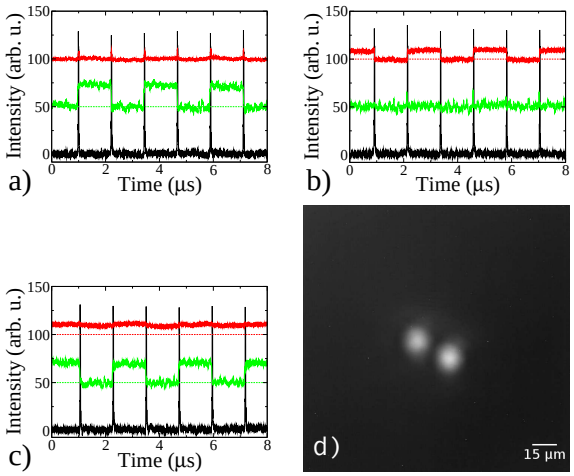

Figure 4. Independent and sequential writing-erasure of one cavity soliton while keeping the neighboring cavity soliton unchanged (Fig.4a,b,c). The black trace corresponds to the incoming localized excitation pulse and the middle (resp. upper) trace, green (resp. red) online, corresponds to the leftmost (resp. rightmost) cavity soliton. The zero intensity levels of the upper and middle traces (dashed lines) have been artificially offset by 100 and 50 respectively for clarity. Differences in the intensity traces for the right and left cavity soliton signals arise because of different gains of the APD. An averaged image of the two cavity solitons considered is shown in d).

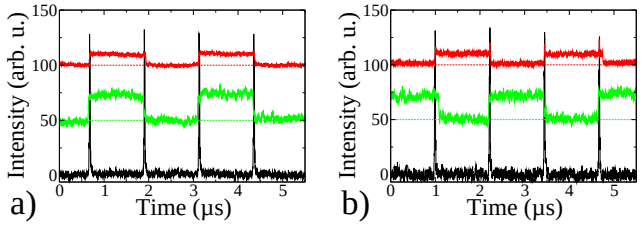

Figure 5. Independent flip-flop operation of the two-cavity solitons shown on Fig.4d) starting from different initial conditions (Fig.5a and b) with one single control beam placed in the middle of the two structures.

least 60µm. And indeed, in Fig. 2e) in [4], we observed two neighbouring structures that we could not manipulate independently. One important point is that in this particular two-spot structure, the distance between the spots was much less than in the present case (the field itself did not go to zero between the two spots) thus giving rise to coupling. In Fig.4d) the two spots are separated by 28μm, more than two CS diametres (12μm FWHM) and the field decreases almost to zero in the region between the two spots. This certainly explains the fact that the two structures are uncoupled. Another coupling mechanism lies in the carrier distributions and in numerical analysis, for standard diffusion coefficients, the lateral size of the localized carrier distributions constituting the CS is of the same order as the one of the field distribution. It is also possible that the numerical modelling underestimates the spatial noise in the system (either because of spontaneous emission or cavity detunings [12]) that prevents the coupling of structures at small distances. Another possible decoupling mechanism could stem from the cavity resonance detuning because of the small wedge in the sample. We should also point out that the formation of CS clusters is still the subject of theoretical [13,14,15] and experimental work [16] and a full comprehension is not yet achieved.

4 Self-pulsing structures

In the following we present several experimental observations of the dynamics associated with single localized states or clusters of localized states. The observations are made in slightly different experimental conditions as in the previous sections. The main two parameters at our disposal are the sample temperature and the location on the sample. The impacts of these parameters on the physical parameters are the following. Firstly, a temperature change will change the cavity resonance wavelength (through the temperature dependence of the index of refraction) and the quantum-wells' band-gaps. Since the rate of change of the band-gap energy and of the optical cavity length are different (typically measured 0.08nm/K in our samples for the latter, larger for the former $\sim$ 0.35nm/K [17]), an additional detuning between the band-gap and the cavity resonance frequencies will appear. This also changes the differential gain and absorption, all the more since we have targeted our quantum wells to have their band-gaps close to the cavity resonance, a region where these parameters strongly depend on detuning. Secondly, due to the fabrication of the sample, a small wedge is introduced over the whole sample that makes the cavity resonance vary. This wedge affects also the quantum wells width but this has a negligible effect on the band-gaps. The cavity resonance tuning range is between 970nm and 995 nm. The local gradient is however non-uniform and varies on the sample surface. It is almost zero at the center of the wafer for a cavity resonance close to 995nm, below 0.3nm/mm in the range 980-995nm and has a maximum of 1.5nm/mm towards the edges of the wafer for short wavelengths.

We observe that self-pulsing is generally favoured close to laser threshold for low heat-sink temperatures (around 0°C or below). It is found here in the whole cavity resonance tuning range. Conversely, bistability can be observed at heat sink temperatures above 0°C and for cavity resonance wavelengths in the 970-980nm range . This can be understood as follows. An increase of the heat sink temperature leads to a stronger linear absorption in the SA section, because the bandgap wavelength will move closer to the cavity resonance. This is confirmed by the fact that we observe an increase of the laser threshold in that case, and if we are in a parameter region where bistability exists, by an increase of the hysteresis cycle width. This behavior is consistent with the results of direct numerical integration of the governing equations ([6]), varying the linear absorption γ. In fact, increasing the laser threshold means that the carrier density at threshold increases (all the more when bimolecular recombination is present), and leads to an increase of the recombination rate of carriers

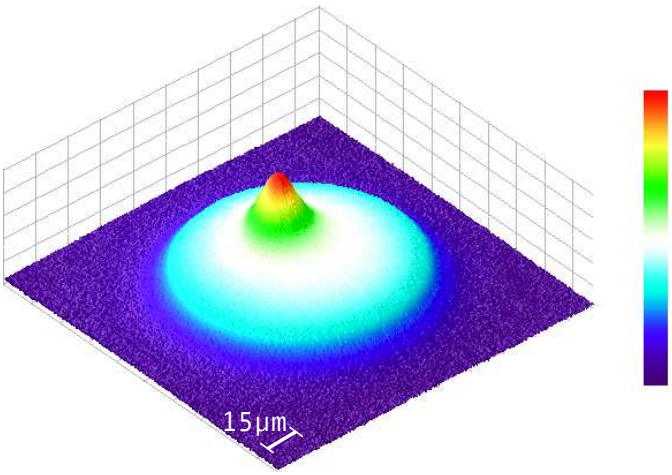

Figure 6. 3D and false color image of the sample surface with a self-pulsing localized state. The large light blue disk is the fluorescence from the ∼90µm pumped area. The dynamics associated with this localized state is shown on Fig.7. The image is an average image integrated over a time much greater than the characteristic time of the dynamics.

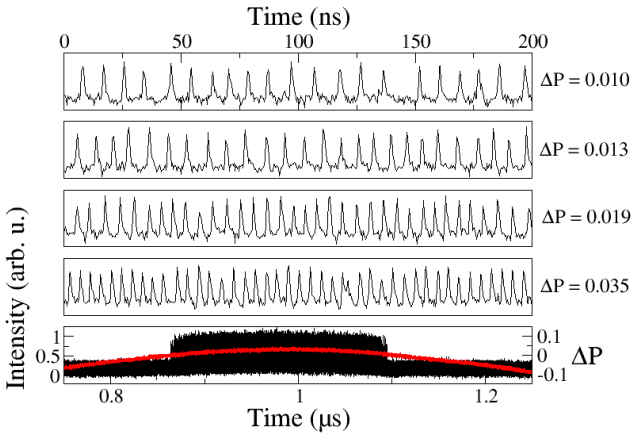

Figure 7. Intensity at the localized state shown in Fig.6 (in black) while slowly modulating the pump (in red) around the threshold pump value P_{th}. Upper graphs display portions of the full time-trace (below) of the pulsing dynamics at various excess pump from threshold $\Delta P = (P - P_{th})/P_{th}$. Pulses of ∼1ns duration with a repetition period ranging from 8.7ns to 4.7ns are clearly identified.

in the gain section. However, since the carrier recombination rate in the SA section is not affected because it is unpumped, the carrier recombination time in the gain section will be much faster than in the SA section. This is known to favour bistability over self-pulsing, as e.g. shown in [18].

In our observations, the dynamical signature of self-pulsing fits well with what we expect from theoretical investigations on self-pulsing in lasers with saturable absorbers [19]. When the pump intensity crosses laser threshold, high intensity pulses are emitted. The onset of pulses corresponds to a homoclinic bifurcation. The intensity of pulses remains almost constant when the pump intensity rises, but the pulses repetition rate increases, starting from zero. At a certain point, oscillations become more harmonic and pulses disappear through a Hopf bifurcation. This sequence has been observed in our experiment. However, the disappearance of self-pulsing through the Hopf bifurcation is sometimes not observed and the system dynamics evolves towards a complex non-stationary state, most probably because of spatio-temporal instabilities.

In most experimental conditions, we can observe self-pulsing without spatial light localisation and light is emitted over a large part of the pumped region. However in smaller regions of parameters, we could observe self-pulsing with light localization as shown in Fig.6. The heat-sink temperature is maintained at $-12.6°C$ and the pump is just above laser threshold. The observation is made with a camera having a long integration time so that the dynamics is averaged on the camera image. The size of the localized structure is ∼ 17µm FWHM and the laser wavelength is 978.72nm. It appears off-centered with respect to the pump beam. The temporal dynamics associated, recorded with a fast APD (90ps rise-time) is shown in Fig.7 while the optical pump is varied sinusoidally at a small rate (1kHz) around the laser threshold. It consists in a train of pulses whose repetition period depends on the pump power and varies between $\gtrsim$10ns to $\lesssim$4ns and whose duration is of the order of 1ns. Self-pulsing starts with high-intensity pulses as expected in the homoclinic bifurcation scenario. This dynamical regime is sensitive to perturbations and in particular to noise present in the system (due to e.g. spontaneous recombination, or pump noise) as we can see on the important jitter present in the pulse repetition rate. Part of this jitter is also due to the fact that the system needs to adjust to the pump change inducing a small equilibrium temperature change in the active zone, and quieter pulsed operation could be obtained with a steady pump. We could not control the state of the self-pulsing, self-localized laser, although it should be possible in principle. The reason why this happens may come from several causes. Firstly, it is not easy to experimentally identify bistability between a self-pulsing state and a non-lasing state in the presence of noise, all the more that the bistable range is small (as expected here [19]). Secondly, it is possible that this observation has to be compared to similar results reported in literature in semiconductor systems [20,21] where cw, localized states where observed and shown not to be controllable (hence not bistable), possibly because of the trapping potential.

Interestingly, at a higher substrate temperature and a slightly different cavity resonance wavelength, we observed bistability between a complex dynamical behaviour and the non-lasing solution. The sample near field is shown on Fig.8. As we show below on Fig.9, the system can either be in the laser-off state or display a complex, irregularly spiking dynamics. It is not yet completely clear whether the dynamics of the total intensity comes from self-pulsing of an inhomogeneous optical structure as a whole in a chaotic regime, or if the dynamics of the individual spots

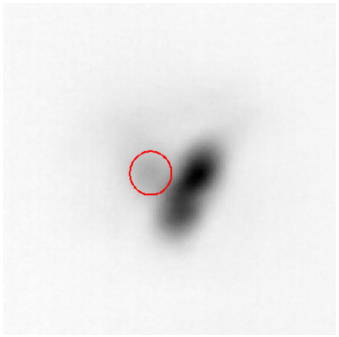

Figure 8. Inverted contrast, averaged CCD camera image of a three-spot cluster displaying a controllable dynamical regime. Heat-sink temperature is -0.3°C and laser light is emitted at 976.78nm. The red circle marks the location of one of the spots that appears weaker than the others.

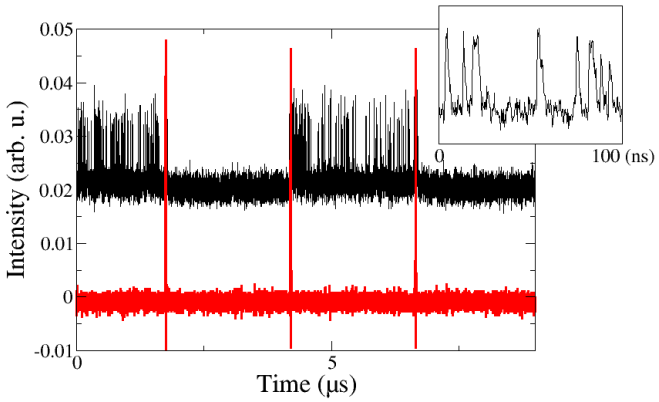

Figure 9. Control of the irregular spiking with an external control beam having 60ps pulse duration and a repetition rate of 400kHz. The whole near-field in Fig.8 is detected on a fast APD (black, and offseted for clarity) and shown with the incoming control pulses in red. The average control beam power is 15mW. In inset is a 100ns duration zoom in the irregular pulsing zone.

is involved. However, pulses can be identified with short durations of the order of 10ns or less.

The same perturbation signal as in previous sections is sent onto the structure. We observe that each time a control pulse is sent, the dynamics is either activated or deactivated. Although noise may by itself trigger some spiking events (possibly outside the controllable area of the structure but inside the detected area), we can observe a very repeatable control that is synchronized with the control pulses. This preliminary result shows nevertheless that it is possible to control dynamical regimes with an external perturbation and is of great interest in the perspective of controlling self-pulsing localized structures predicted to exist in microlasers with saturable absorbers in [8].

5 Conclusion

We have reported the observation and control of laser cavity solitons in a monolithic vertical-cavity laser with saturable absorber. We have described the original sample design and the fabrication process. Independent and successive control over two structures is obtained thanks to a unique control beam. With the same sample while in slightly different parameter ranges, but we could observe localized self-pulsing as well as a more complex spatio-temporal dynamical state that we could control with an external perturbation. We believe these results are encouraging in the perspective of having a source of controllable self-pulsing cavity solitons.

This work was partially realized in the framework of the European STREP project FUNFACS (www.funfacs.org). We thank X. Hachair for his critical reading of the manuscript.

References

1. X. Hachair, F. Pedaci, E. Caboche, S. Barland, M. Giudici, J. Tredicce, F. Prati, G. Tissoni, R. Kheradmand, L. Lugiato et al., IEEE J. Sel. Topics in Quantum Electron. **12**, 339 (2006)
2. P. Genevet, S. Barland, M. Giudici, J.R. Tredicce, Phys. Rev. Lett. **101**(12), 123905 (2008)
3. Y. Tanguy, T. Ackemann, W. Firth, R. Jï¿œger, Phys. Rev. Lett. **100**, 013907 (2008)
4. T. Elsass, K. Gauthron, G. Beaudoin, I. Sagnes, R. Kuszelewicz, S. Barbay, Appl. Phys. B **98**, 327 (2010)
5. M. Bache, F. Prati, G. Tissoni, R. Kheradmand, L. Lugiato, I. Protsenko, M. Brambilla, Appl. Phys. B **81**, 913 (2005)
6. F. Prati, P. Caccia, G. Tissoni, L. Lugiato, K. Mahmoud Aghdami, H. Tajalli, Appl. Phys. B **88**, 405 (2007)
7. A.G. Vladimirov, S.V. Fedorov, N.A. Kaliteevskii, G.V. Khodova, N.N. Rosanov, J. Opt. B **1**, 101 (1999)
8. N.N. Rozanov, S.V. Fedorov, A.N. Shatsev, Opt. Spectrosc. **91**, 232 (2001)
9. S. Lim, J. Hudgings, G. Li, W. Yuen, K. Lau, C. Chang-Hasnain, Elec. Lett. **33**, 1708 (1997)
10. A.J. Fischer, W.W. Chow, K.D. Choquette, A.A. Allerman, K.M. Geib, Appl. Phys. Lett. **76**, 1975 (2000)
11. S. Barbay, Y. Mï¿œnesguen, I. Sagnes, R. Kuszelewicz, Appl. Phys. Lett. **86**, 151119 (2005)
12. R. Kuszelewicz, I. Ganne, I. Sagnes, G. Slekys, M. Brambilla, Phys. Rev. Lett. **84**, 6006 (2000)
13. G. Kozyreff, P. Assemat, S.J. Chapman, Phys. Rev. Lett. **103**, 164501 (2009)
14. N. Rosanov, S. Fedorov, A. Shatsev, Appl. Phys. B **81**, 937 (2005)
15. N. Rosanov, S. Fedorov, A. Shatsev, J. Exp. Theor. Phys. **98**(3), 427 (2004)
16. S. Barbay, X. Hachair, T. Elsass, I. Sagnes, R. Kuszelewicz, Phys. Rev. Lett. **101**, 253902 (2008)
17. J. Botha, A.W.R. Leitch, Journal of Electronic Materials **29**, 1362 (2000)
18. H. Kawaguchi, Appl. Phys. Lett. **45**(12), 1264 (1984)
19. J.L.A. Dubbeldam, B. Krauskopf, Opt. Commun. **159**, 325 (1999)
20. Y. Mï¿œnesguen, S. Barbay, X. Hachair, L. Leroy, I. Sagnes and R. Kuszelewicz, Phys. Rev. A **74**, 023818 (2006)
21. X. Hachair, S. Barland, L. Furfaro, M. Giudici, S. Balle, J. R. Tredicce, M. Brambilla, T. Maggipinto, I. M. Perrini, G. Tissoni, L. Lugiato, Phys. Rev. A **69**, 043817 (2004)